Research in Astron. Astrophys. **2011** Vol. **11** No. **7**, 833–842
http://www.raa-journal.org *http://www.iop.org/journals/raa*

Research in Astronomy and Astrophysics

Spectroscopic and photometric observations of unidentified ultraviolet variable objects in the GUVV-2 Catalog *

You Li[1,2], Jing Wang[2], Jian-Yan Wei[2] and Xiang-Tao He[1]

[1] Department of Astronomy, Beijing Normal University, Beijing, 100875, China; *ollie-321@hotmail.com*
[2] National Astronomical Observatories, Chinese Academy of Sciences, Beijing 100012, China

Received 2010 December 31; accepted 2011 March 24

Abstract An NUV-optical diagram composed from sources from the second Galaxy Evolution Explorer (GALEX) Ultraviolet Variability (GUVV-2) Catalog provides us with a method to tentatively classify the unknown GUVV-2 sources by their NUV-optical magnitudes. For the purpose of testing the correctness and generality of the method, we carry out a program on the spectroscopic observations of the unidentified GUVV-2 sources. The spectroscopic identification of these 37 sources are 19 type -A to -F stars, 10 type -G to -K stars and 7 M dwarf stars together with an AGN. We also present the light curves in the R-band for two RR Lyrae star candidates selected from the NUV-optical diagram, both of which undergo cyclic variations. Combining their light curves and colors, we classify them as RR Lyrae stars. To confirm the results, we show a color-color diagram for the 37 newly identified spectroscopic objects compared with previously identified ones, which are consistent with our previous results, indicating that the ultraviolet variable sources can initially be classified by their NUV/optical color-color diagram.

Key words: stars: variables: general — galaxies: active — methods: observational — ultraviolet emission

1 INTRODUCTION

The NASA *Galaxy Evolution Explorer* (GALEX) satellite (Martin et al. 2005) is an ongoing mission with the aim of studying star formation in galaxies and their evolution over time in ultraviolet bands. A modified Ritchey-Chretien telescope with a diameter of 50 cm and a field-of-view of 1.2° is used to image and spectroscopically observe the sky in two ultraviolet bands (NUV 1750–2750 Å, FUV 1350–1750 Å) down to an AB magnitude of $m_{\rm AB} \sim 25$ m in the deepest modes (Morrissey et al. 2007). So far, it has imaged 2/3 of the sky[1] during its All-sky Imaging Survey (AIS), Medium Imaging Survey (MIS) and Deep Imaging Survey (DIS) since its launch on 2003 April 28.

Repeated observation of selected areas of the sky enables FUV and NUV fluxes at many different epochs to be determined for numerous sources. Thus, variable ultraviolet sources can be detected,

∗ Supported by the National Natural Science Foundation of China.

[1] The GALEX pointings are kept away from the Galactic plane and the Magellanic clouds in order to avoid damage to its detector caused by bright stars ($\sim$ 10th magnitude).

many of which exhibit much larger amplitudes of variation in the ultraviolet region than that typically found at visible wavelengths (Wheatley et al. 2008).

In addition to the shallow survey, GALEX repeatedly performed deeper image observations for the selected sky area. The repeated observations in DIS and MIS allowed Welsh et al. (2005) to release the first GALEX ultraviolet variability catalog (GUVV-1), which contains 84 variable and transient UV sources obtained during the first 15 months of the GALEX AIS. M dwarf flare stars and ab-type RR Lyrae stars are the largest ultraviolet variable objects detected by GALEX in GUVV-1 (Welsh et al. 2005). The sample was subsequently enlarged to the second version (GUVV-2, Wheatley et al. 2008) by the repeated observations in DIS and in certain Guest Investigator (GI) observations.

GUVV-2 contains 410 variable sources obtained during the period 2003 June – 2006 June. About 72% of the sources in GUVV-2 had not been spectroscopically identified at that time. The previously identified objects from the SIMBAD catalog in GUVV-2 are mainly quasars/AGNs (77), RR Lyrae stars (6), dMe stars (2) and X-ray binaries (19).

We systematically performed follow-up optical spectroscopic and photometric observations for the unknown sources listed in the GUVV-2 catalog. In this paper, we provide a method to tentatively classify ultraviolet variable sources into several common source types by their NUV-optical color-color diagram. This method is confirmed by our spectroscopic and photometric observations. We report results of the spectroscopic identification for 37 previously unknown sources. Photometric monitoring was carried out on two unidentified RR Lyrae star candidates to confirm their variability through their light curves. The paper is organized as follows. Section 2 presents the motivations, observations and data reductions. The results and discussions are given in Section 3 and Section 4, respectively, and are followed by the conclusion.

2 MOTIVATIONS, OBSERVATIONS AND DATA REDUCTION

2.1 Motivations

In GUVV-2, among the 114 sources with previous SIMBAD catalog identifications, there are mainly three common types: quasars/AGNs, RR Lyrae stars and M dwarf stars. In order to statistically analyze the spectral types of GUVV-2 sources, we have produced a color-color diagram for them using their NUV magnitudes and optical magnitudes of B2 and R2 from the USNO-B1.0 catalog (Monet et al. 2003, Fig. 1).

The sources contained in this diagram are previously known quasars/AGNs, RR Lyrae stars, M dwarf stars and unidentified cases. The plot of ($\mathrm{NUV_{max}}$–B2) versus (B2–R2) reveals that the sources are segregated into different isolated regions according to their spectral types. The AGNs are mainly clustered at the bottom-left corner because of their non-thermal blue spectrum and strong NUV emissions from the hot disk around the central supermassive black hole. The RR Lyrae stars are located within the region at the right of the AGNs because of the strong Balmer jumps. The M dwarf stars are located at the top-right end of the diagram simply because of their low stellar surface temperature. The distribution of these previously known sources allows us to select the candidates for the unknown sources with different types by their NUV-optical colors.

To preliminarily test the results, we have chosen two RR Lyrae star candidates from the region where RR Lyrae stars are located to perform photometric monitoring. These two sources are also selected as RR Lyrae star candidates by their SDSS magnitudes (Wheatley et al. 2008).

Taking account of the poor sample of the overlapping GUVV-2-SIMBAD sources and their potential bias, we have performed further spectroscopic observations for the randomly chosen unknown sources in GUVV-2 to verify the correctness and generality of this method.

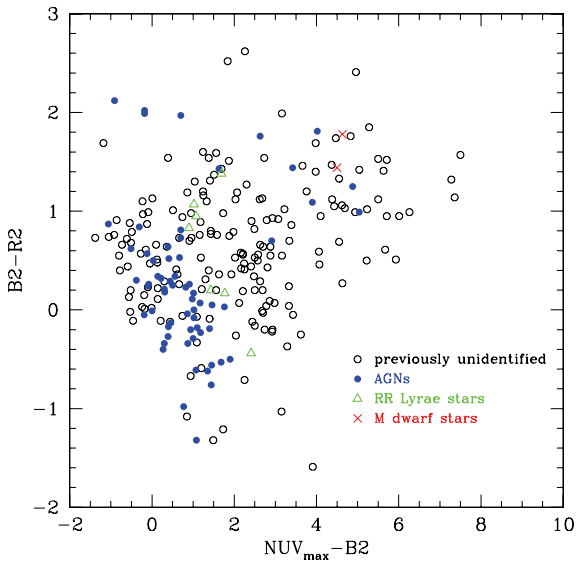

Fig. 1 Plot of ($\mathrm{NUV_{max}} - \mathrm{B2}$) vs. (B2–R2) for previously identified variable sources. The filled circles in blue, open triangles in green, crosses in red are previously identified AGNs, RR Lyrae stars and M dwarf stars, respectively. The black open circles have no current identifications (color online).

2.2 Spectroscopic Observations

We only carried out spectroscopic observations of the unidentified GUVV-2 sources with B-band magnitudes brighter than 17.5 mag and declination $> -15^{\circ}$ due to the constraint of the observatory site and the instrumental capability. Based on the limitation of our observing time, sources were chosen according to their suitable right ascension in every run of our observations. This principle resulted in a list of 37 unidentified sources to be observed (Table 1).

The spectroscopic observations were performed during several observing runs between 2009 and 2010 using the National Astronomical Observatories, Chinese Academy of Sciences (NAOC) 2.16 m telescope at the Xinglong observing station. The observations were taken with an OMR spectrograph attached to the Cassegrain focus, and a back-illuminated SPEC10 1024×400 CCD camera employed as the detector. A grating of 300 g mm^{-1} and a slit of around $2.0''$ oriented in the south-north direction were used. This setup results in a final spectral resolution of $\sim$9 Å as measured from both comparison spectra and night sky emission lines. The spectroscopic observation log for the identified objects is listed in Table 1.

The wavelength calibrations were carried out by the He/Ne/Ar comparison arcs taken several times during each observation run. Two or three Kitt Peak National Observatory (KPNO) standard stars (Massey et al. 1988) were observed per night for flux calibration.

The raw data were bias subtracted and flat-field corrected, and cosmic-rays were removed using the IRAF package[2]. The one-dimensional sky-subtracted spectra were then wavelength and flux calibrated. The uncertainties in the wavelength and flux calibrations are no more than 1Å and 20%, respectively.

[2] IRAF is distributed by the National Optical Astronomy Observatory, which is operated by the Association of Universities for Research in Astronomy, Inc., under cooperative agreement with the National Science Foundation; *http://iraf.noao.edu.*

Table 1 Observation Log for the Identified Objects

GALEX ID (1)	α (J2000.0) (2)	δ (J2000.0) (3)	$N_{\rm det}$ (4)	$\rm NUV_{max}$ (5)	ΔNUV (6)	B2 (7)	R2 (8)	I (9)	Obs. Date (10)	Exposure (s) (11)	Spectral Type (12)
J002442.4+165808.0	00 24 42.52	+16 58 06.4	8	17.68	0.71	13.62	13.03	12.67	Oct. 14 2009	900	F
J004215.3+200957.3	00 42 15.36	+20 09 59.8	15	18.94	1.65	13.88	12.35	11.08	Oct. 14 2009	900	G
J013642.0–062743.1	01 36 42.03	–06 27 43.8	10	19.70	0.63	16.79	16.31	16.12	Oct. 14 2009	2400	A
J021547.1–045207.8	02 15 47.14	–04 52 08.2	7	19.60	0.67	15.06	12.96	12.37	Sep. 21 2009	900	G
J022003.0-032910.7	02 20 03.08	–03 29 10.1	7	20.01	0.73	16.19	14.44	13.77	Oct. 14 2009	1800	K
J022050.6–061528.0	02 20 50.71	–06 15 28.4	7	18.99	0.77	14.67	13.14	12.24	Sep. 21 2009	900	G
J042733.6+165222.2	04 27 33.67	+16 52 21.8	5	20.18	0.73	16.34	14.90	12.93	Jan. 23 2010	900	M
J042832.3+165821.6	04 28 32.37	+16 58 21.2	7	19.30	1.64	16.60	15.96	14.90	Jan. 23 2010	1800	F
J043431.2+172220.1	04 34 31.28	+17 22 20.2	13	19.66	0.71	17.22	15.05	14.36	Jan. 25 2010	2400	M
J081226.4+033320.5	08 12 26.37	+03 33 20.4	77	18.95	1.95	17.26	15.88	16.00	Jan. 25 2010	3600	F
J090853.4–021242.8	09 08 53.48	–02 12 43.2	13	19.23	0.98	15.90	15.66	16.16	Nov. 10 2010	3600	F
J091332.6-101108.2	09 13 32.65	–10 11 08.1	15	19.11	1.47	15.35	14.15	13.46	Nov. 10 2010	2400	AGN
J095847.6+021815.3	09 58 47.64	+02 18 15.1	11	18.62	1.42	14.59	13.54	13.03	Mar. 12 2010	1200	F
J102841.9+570840.4	10 28 41.94	+57 08 40.1	24	18.27	1.26	14.01	12.85	12.49	Mar. 15 2010	900	G
J102911.8+575806.1	10 29 11.81	+57 58 05.5	18	19.54	1.13	11.52	9.78	8.96	Mar. 15 2010	600	M
J103538.2+581549.1	10 35 38.19	+58 15 49.2	20	15.53	1.92	13.59	12.96	12.24	Mar. 15 2010	700	A
J120519.8–075605.6	12 05 19.83	–07 56 06.1	31	19.63	1.19	15.20	13.41	12.58	Mar. 13 2010	1200	K
J123523.7+614132.4	12 35 23.71	+61 41 31.9	92	20.34	0.61	14.50	13.48	12.84	Mar. 13 2010	900	K
J123718.3+624207.9	12 37 18.39	+62 42 07.9	29	20.23	0.75	13.89	12.18	10.81	Jan. 23 2010	2400	M
J132602.6+273502.3	13 26 02.68	+27 35 02.1	70	17.40	3.33	14.66	12.10	10.55	Jan. 23 2010	1800	M
J143126.4+342710.3	14 31 26.36	+34 27 10.4	18	18.40	0.86	13.78	12.72	11.68	Mar. 15 2010	600	G
J145110.3+310639.8	14 51 10.45	+31 06 40.7	24	18.72	0.86	13.58	11.24	9.78	Mar. 15 2010	600	M
J160902.8+524224.4	16 09 02.81	+52 42 24.4	18	19.11	0.74	17.36	18.00	17.44	Oct. 05 2010	3600	A
J163853.2+413932.7	16 38 53.25	+41 39 36.1	29	19.97	1.02	12.33	11.34	10.93	Oct. 06 2010	300	K
J163952.7+420951.6	16 39 52.77	+42 09 52.0	19	18.29	1.75	15.79	15.95	15.64	Oct. 05 2010	1200	A
J171250.9+582748.6	17 12 50.87	+58 27 48.4	14	18.51	0.63	16.06	15.74	15.40	Oct. 06 2010	900	A
J172033.4+585513.2	17 20 33.51	+58 55 13.5	37	20.12	0.80	15.12	14.34	14.13	Oct. 06 2010	900	G
J194443.4–074959.5	19 44 43.40	–07 49 59.4	11	19.85	0.76	15.08	12.90	11.36	Sep. 20 2009	600	M
J194704.9–075446.1	19 47 04.99	–07 54 47.0	7	19.56	1.43	16.78	16.74	16.32	Jun. 30 2009	1800	F
J203922.4–010346.0	20 39 22.45	–01 03 46.1	19	16.88	0.81	14.54	14.04	13.39	Sep. 21 2009	600	A
J203958.8–010714.3	20 39 58.85	–01 07 14.6	19	18.43	1.20	16.33	14.93	14.36	Oct. 06 2010	1200	F
J204024.3–010950.0	20 40 24.30	–01 09 50.7	15	19.06	0.72	16.53	16.29	15.35	Jun. 30 2009	1800	F
J204114.7–005220.9	20 41 14.80	–00 52 21.0	19	19.59	1.38	17.69	16.50	15.96	Jun. 30 2009	1800	F
J214909.5–050558.6	21 49 09.51	–05 05 59.1	26	18.67	2.28	17.29	16.89	16.50	Oct. 13 2009	2400	F
J223601.0+134711.5	22 36 01.10	+13 47 11.2	27	19.16	0.91	16.78	16.00	14.59	Oct. 06 2010	2400	A
J224029.0+120056.3	22 40 29.01	+12 00 55.7	19	17.56	0.85	15.73	14.59	14.37	Oct. 05 2010	1200	A
J224143.6+115326.2	22 41 43.67	+11 53 25.4	14	17.08	1.27	14.27	14.18	13.91	Oct. 14 2009	1200	A

Notes: Cols. (2)–(3) list the right ascension (J2000.0) and corresponding declination (J2000.0) of the objects given by 2MASS except GALEX J160902.8+524224.4 which is given by SDSS; Col. (4) lists the total number of detections ($N_{\rm det}$) of the variable sources, Col. (5) lists the maximum NUV magnitude for the source (measured in a single exposure) and Col. (6) lists the variation between the corresponding maximum and minimum NUV magnitudes; Cols. (7)–(9) list the photometric magnitudes of B2, R2 and I given by USNO-B1.0.

2.3 Photometric Observations

To confirm the results, on the basis of our observing time, we have chosen two unidentified RR Lyrae star candidates from the region where RR Lyrae stars are located on the NUV-optical diagram with suitable brightness and right ascension to perform photometric monitoring. These two sources (GALEX J100133.2+014328.5 and GALEX J155800.6+535233.6) are also selected as RR Lyrae star candidates by their SDSS magnitudes (Wheatley et al. 2008). Each of the two sources was monitored using the 85 cm NBT telescope at Xinglong station of NAOC for two days from 2010 March 09 to 2010 March 10. A standard Johnson-Cousin-Bessel system was mounted at the primary focus of the telescope. A PI1024 BFT 1024×1024 CCD was used as the detector. The field-of-view was about $16.5 \times 16.5\ \rm arcmin^2$ at a focal ratio of 3.27 (f=2780 mm), which resulted in an image scale

of $0.96''$ per pixel (Zhou et al. 2009). Standard Johnson V- and R-band filters were used during our observations. The typical exposure times for the V- and R-band filters were 800 s and 600 s, respectively. In all of the observations, the sky flat-field frames in U, V and R passbands were obtained before and after each observation run during twilight.

The raw CCD images were preliminarily reduced using the standard CCDPROC routines in the IRAF package. For the purpose of differential photometry, we first chose several bright stars observed with good seeing from the same CCD frame as the comparison stars. Then, some check stars with brightness comparable to the object were selected to assess any photometry errors. Aperture photometry was adopted in order to calculate the instrumental magnitudes of the objects and the selected stars by the APPHOT task in the IRAF package.

3 RESULTS AND DISCUSSIONS

3.1 Spectroscopic Identification

The observed one-dimensional spectra are visually classified into various types. The spectral types are listed in Col. (12) in Table 1. All the observed sources are classified as stars except for one AGN (i.e., GALEX J091332.6–101108.2). The spectrum of that object is shown in Figure 2. The spectrum of GALEX J091332.6–101108.2 shows a strong broad Hα emission line, but a very weak and even undetectable broad Hβ component, which allows us to classify the object as a Seyfert 1.9 galaxy rather than a typical type I AGN. The redshift is inferred to be $z = 0.055$ according to the Hα emission line. The continuum of the object is dominated by the stellar absorption features emitted from the host galaxy, which means that the object is not included in the quasar candidates selected from the GUVV-2 catalog through their colors by Wheatley et al. 2008.

GALEX NUV and FUV observations are found to be sensitive probes for the variability of RR Lyrae stars. The flux variability in RR Lyrae stars results from the radial pulsations that cause a cyclic temperature variation due to stellar surface contraction and expansion. Out of the total 37 objects, 19 objects show spectra typical of type -A to -F stars due to their strong Balmer absorption features and Balmer jumps. A typical spectrum is presented in Figure 3 as an illustration.

Figure 4 shows the distribution of NUV magnitude variability for these identified type -A to -F stars. All the type -A to -F stars have large NUV magnitude variability. The average and median values are 1.22 and 1.20 mag, respectively, which are typical of the variability of RR Lyrae stars (Wheatley et al. 2005).

Seven M dwarf stars are identified in our spectroscopic observations. The spectra of the seven M dwarf stars are presented in Figure 5. Five of them were active during our observations because

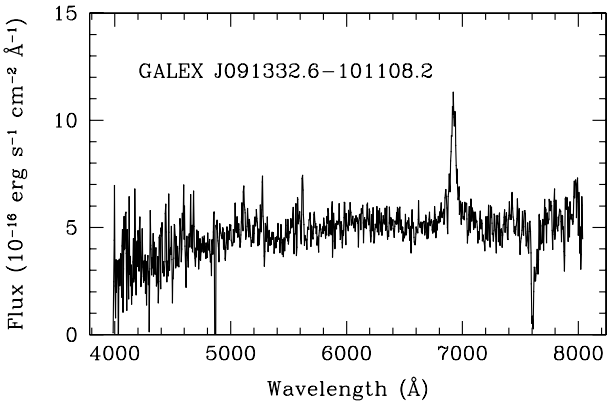

Fig. 2 Spectrum of the newly identified AGN: GALEX J091332.6–101108.2.

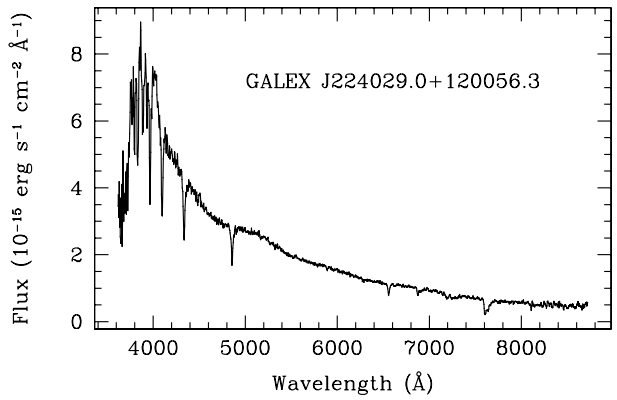

Fig. 3 A typical spectrum of the newly identified A-type star.

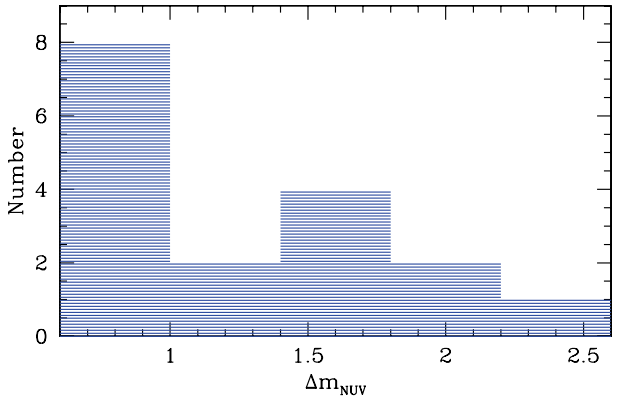

Fig. 4 Distribution of the $\Delta m_{\rm NUV}$ for the newly identified type -A to -F stars.

of the detected Hα emission line. M dwarf flare (dMe) stars are believed to be associated with coronal activity caused by their strong magnetic field coupled with stellar disks (see review in Haisch et al. 1991). The flares last from seconds to hours in X-ray, ultraviolet, optical and radio bands (e.g., Schmitt et al. 1993; Stepanov et al. 1995; Phillips et al. 1988; Welsh et al. 2006). Although the physics of these flares is still poorly understood at present, it is widely believed that the UV flare emission in dMe stars is produced by hot gas with a temperature of 10^5 K located in the chromosphere. In addition to the flare events, the coronal activity of dMe stars can also be spectroscopically identified according to their strong Balmer emission lines, especially Hα (e.g., Worden & Peterson 1976; Shkolnik et al. 2011).

Unlike the other six M dwarf stars, the source (GALEX J123718.3+624207.9) has a spectrum of an extreme early type ($\sim$M0) M dwarf star (see Fig. 4). We attempt to quantitatively determine the spectral types of the other six M dwarf stars using the comprehensively studied spectral indices that are now widely used to produce quantitative spectral classifications of M dwarfs according to the red part of their spectra (i.e., 6300–9000 Å, e.g., Reid et al. 1995; Kirkpatrick et al. 1995; Martín et al. 1999; Hawley et al. 2002). Each index is defined as the ratio between the mean flux in the pseudo-continuum bands and the molecular band. Taking into account the resolution of our spectra, the spectral indices used include: TiO5, CaH2, CaH3 (Reid et al. 1995), TiO7140 (Wilking et al. 2005), VO2 (Lépine et al. 2003), and C81 (Stauffer et al. 1999). The values of the spectral indices

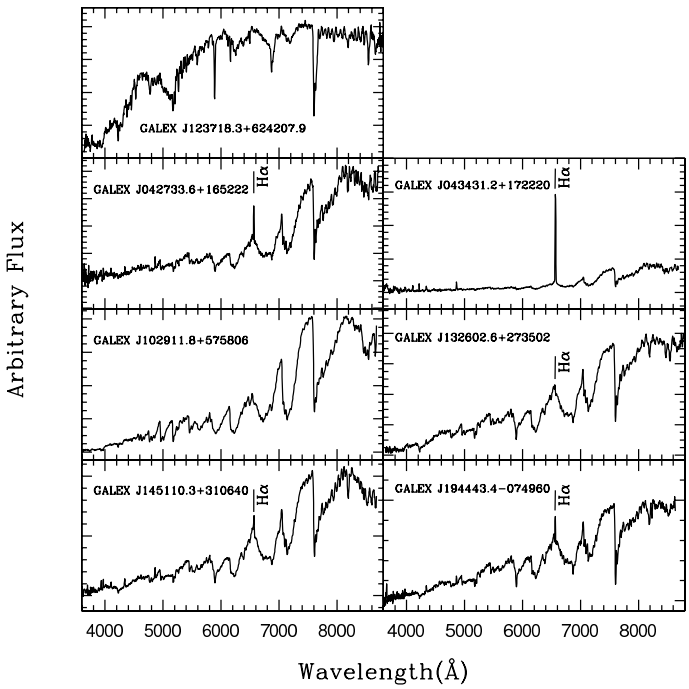

Fig. 5 Spectra of seven newly discovered M dwarf stars.

Table 2 M Dwarf Stars: Spectral Types and Corresponding Spectral Indices

GALEX Name	TiO 5	CaH 2	CaH 3	TiO 7140	VO 2	C81	Spectral type
J042733.6+165222	0.415	0.411	0.681	1.783	0.746	1.275	M3.78
J043431.2+172220	0.456	0.441	0.724	1.807	0.685	1.400	M3.70
J102911.8+575806	0.389	0.492	0.889	2.358	0.755	1.368	M3.61
J132602.6+273502	0.535	0.510	0.787	1.555	0.832	1.160	M2.63
J145110.3+310640	0.531	0.446	0.713	1.646	0.816	1.286	M3.22
J194443.4−074960	0.499	0.490	0.735	1.495	0.892	1.107	M2.71

are calculated for all of the objects using the *SPLOT* task in the IRAF package and are listed in Table 2. Our spectral type determination indicates that the spectral types calculated by different indices are generally consistent with each other within an uncertainty of about one sub-type for an individual object. The determined average spectral types are listed in the last column in Table 2.

3.2 Cyclic Light Curves

We monitored two RR Lyrae star candidates without spectroscopic identification, GALEX J100133.2+014328.5 and GALEX J155800.6+535233.6 in optical V- and R-bands. Both of the light curves in the R-band are presented in Figure 6. Cyclic variations can be identified from the light curves for both objects, although the light curves are under-sampled. For GALEX J100133.2+014328.5, the light curve during the first night covers not only the peak, which is confirmed by the observation taken the next day, but also the following valley. The Phase Dispersion Minimization (PDM) method yields a period of roughly 0.54 d. Given the light curve obtained in the first night, the R-band flux variability in the objects is as large as 1 mag, which is consistent with

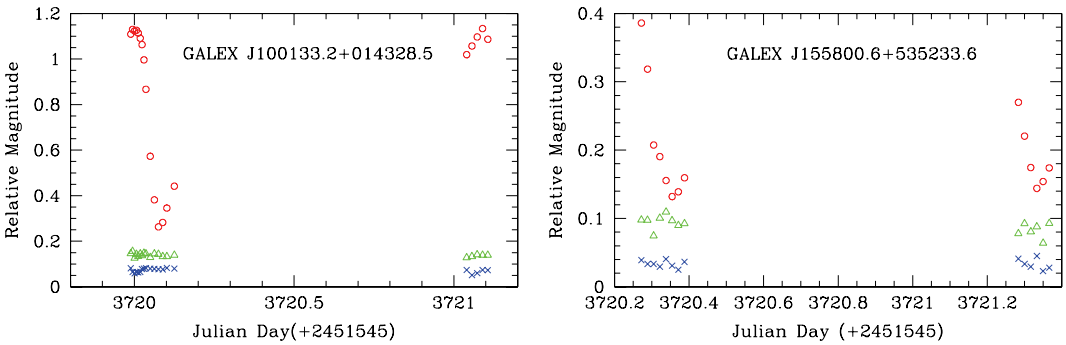

Fig. 6 Light curves of two RR Lyrae star candidates.

the typical value of RR Lyrae stars (Skillen et al. 1993). Although the valley in the light curve is covered twice in GALEX J155800.6+535233.6, the peak in the light curve is missed in our observations because of the under-sampling. The poor sampling prevents us from obtaining a period by the PDM method. The amplitudes of the NUV band of GALEX J100133.2+014328.5 and GALEX J155800.6+535233.6 are 1.98 and 0.87, respectively, which are much larger than the amplitude of the optical band. Combining the colors, cyclic light curves and amplitude of the ultraviolet and optical band allow us to classify the two objects as RR Lyrae stars, which preliminarily demonstrates the result of the color-color diagram.

3.3 Color-Color Diagram

In order to confirm the generality of the results derived from Figure 1, we compare the new spectroscopically identified objects with the previously identified ones in the NUV-optical color-color diagram (Fig. 7).

The type -A to -F stars and M dwarf stars are clustered together with the previously identified RR Lyrae stars and M dwarf stars, respectively, which show good consistency with the results from Figure 1. Between the regions of type -A to -F stars and M dwarf stars, there are some type -G to -K stars which may be solar-like coronal active stars, further confirming the distribution trend of sources with a different energy spectrum. Only one AGN (marked as a large blue open star) is classified as a Seyfert 1.9 galaxy, whose location is consistent with its continuum dominated by the stellar absorption features emitted from the host galaxy.

3.4 Statistics of the Identified Sources

There are a total of 150 sources containing two parts, which are newly identified spectroscopic sources and sources with previous SIMBAD identifications, respectively. The statistics of all the identified sources of different types are listed in Table 3.

Table 3 Statistics of all the Identified Sources

AGNs (1)	RR Lyrae stars/Type A-F stars (2)	Type G-K stars (3)	M dwarf stars (4)	X-binaries (5)	Others (6)	Total (7)
78	25	10	9	19	9	150
52 %	16.7%	6.7%	6%	12.7%	6%	100%

Notes: Column (2) lists the previously identified RR Lyraes together with the newly identified type -A to -F stars.

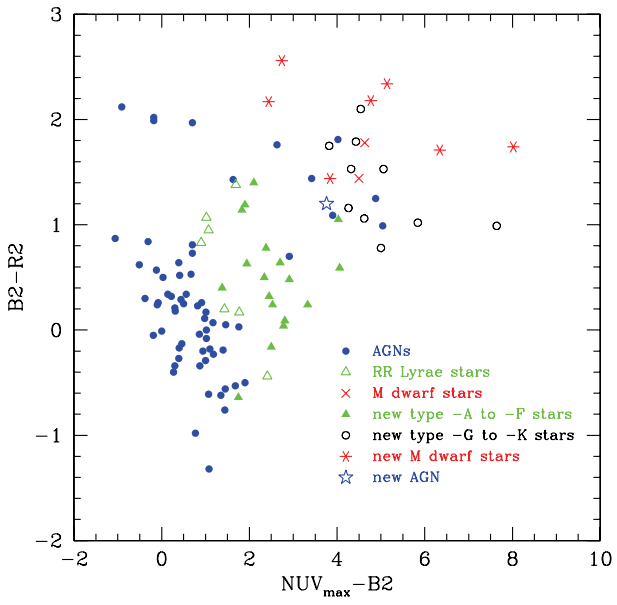

Fig. 7 Plot of ($\mathrm{NUV_{max}} - \mathrm{B2}$) vs. (B2 – R2) for the new spectroscopically identified objects compared with the previously identified ones. The filled triangles in green, open circles in black, snowflake shape in red are newly discovered type -A to -F stars, type -G to -K stars and M dwarf stars, respectively; the large blue star is a newly discovered AGN. The previously identified sources are similarly marked as in Fig. 1.

4 CONCLUSIONS

We have made an NUV-optical color-color plot for the previously known sources and the unidentified ones in GUVV-2, which separate sources into different regions. The identified sources in each region correspond to a certain spectral type, which allows us to tentatively classify the unknown sources simply by their NUV and optical magnitudes. Using this method, we chose two initially classified RR Lyrae star candidates to perform photometric monitoring, and their NUV and optical amplitude together with their cyclic light curves allow us to finally classify them as RR Lyrae stars. We have also carried out spectroscopic observations of 37 randomly chosen unknown GUVV-2 sources. There are seven M dwarf flare stars and an AGN. Five of the M dwarf stars were active during our observations because of their Hα emission. The AGN shows a strong broad Hα emission line, but a very weak and even undetectable broad Hβ component, which allows us to classify the object as a Seyfert 1.9 galaxy rather than a typical type I AGN. The other sources are stars with spectral types from A to K. The location of all these newly identified sources on the NUV-optical diagram shows good consistency with previously known sources, which confirms the correctness and generality of the initial classifications. Thus, at least for our results, we can rapidly and effectively classify the unknown ultraviolet variable sources into several spectral types by their NUV and optical magnitudes.

Acknowledgements JW and JYW are supported by the National Basic Research Program of China (Grant 2009CB824800). JW is funded by the National Natural Science Foundation of China (Grant No. 10803008). We would like to thank the anonymous referee for very useful comments and important suggestions that improved the paper. This work was partially supported by the Open Project

Program of the Key Laboratory of Optical Astronomy, NAOC, CAS. We thank Feng Qichen and Bai Yu for their share of observing time. Special thanks go to the staff at Xinglong observing station, which is part of NAOC, CAS, for their instrumental and observational help.

References

Haisch, B., Strong, K. T., & Rodono, M. 1991, ARA&A, 29, 275
Hawley, S. L., Covey, K. R., Knapp, G. R., et al. 2002, AJ, 123, 3409
Kirkpatrick, J. D., Henry, T. J., & Simons, D. A. 1995, AJ, 109, 797
Lépine, S., Rich, R. M., & Shara, M. M. 2003, AJ, 125, 1598
Martin, D. C., Fanson, J., Schiminovich, D., et al. 2005, ApJ, 619, L1
Martín, E. L., Delfosse, X., Basri, G., et al. 1999, AJ, 118, 2466
Massey, P., Strobel, K., Barnes, J. V., & Anderson, E. 1988, ApJ, 328, 315
Monet, D. G., Levine, S. E., Canzian, B., et al. 2003, AJ, 125, 984
Morrissey, P., Conrow, T., Barlow, T. A., et al. 2007, ApJS, 173, 682
Phillips, K. J. H., Bromage, G. E., Dufton, P. L., Keenan, F. P., & Kingston, A. E. 1988, MNRAS, 235, 573
Reid, I. N., Hawley, S. L., & Gizis, J. E. 1995, AJ, 110, 1838
Schmitt, J. H. M. M., Haisch, B., & Barwig, H. 1993, ApJ, 419, L81
Shkolnik, E. L., Liu, M. C., Reid, I. N., Dupuy, T., & Weinberger, A. J. 2011, ApJ, 727, 6
Skillen, I., Fernley, J. A., Stobie, R. S., & Jameson, R. F. 1993, MNRAS, 265, 301
Stauffer, J. R., Barrado y Navascués, D., Bouvier, J., et al. 1999, ApJ, 527, 219
Stepanov, A. V., Fuerst, E., Krueger, A., et al. 1995, A&A, 299, 739
Welsh, B. Y., Wheatley, J., Browne, S. E., et al. 2006, A&A, 458, 921
Welsh, B. Y., Wheatley, J. M., Heafield, K., et al. 2005, AJ, 130, 825
Wheatley, J. M., Welsh, B. Y., & Browne, S. E. 2008, AJ, 136, 259
Wheatley, J. M., Welsh, B. Y., Siegmund, O. H. W., et al. 2005, ApJ, 619, L123
Wilking, B. A., Meyer, M. R., Robinson, J. G., & Greene, T. P. 2005, AJ, 130, 1733
Worden, S. P., & Peterson, B. M. 1976, ApJ, 206, L145
Zhou, A., Jiang, X., Zhang, Y., & Wei, J. 2009, Research in Astronomy and Astrophysics, 9, 349